# Second harmonic generation in the plasmon-polariton gap of quasiperiodic metamaterial photonic superlattices

F. Reyes Gómez,[1,2] N. Porras-Montenegro,[1] Osvaldo N. Oliveira Jr.,[3] and J. R. Mejía-Salazar[3,4,*]

[1]*Physics Department, del Valle University, AA 25360, Cali, Colombia*

[2]*Department of Applied Physics, University of Cantabria, Avda. Los Castros, s/n, 39005 Santander, Spain*

[3]*São Carlos Institute of Physics, University of São Paulo, CP 369, 13560-970, São Carlos, SP, Brazil*

[4]*National Institute of Telecommunications (Inatel), 37540-000, Santa Rita do Sapucaí, MG, Brazil*

(Received 27 March 2018; published 7 August 2018)

Self-similar bulk plasmon-polariton modes in quasiperiodic photonic superlattices were used here for a giant enhancement of second harmonic generation. Results for Fibonacci and Thue-Morse-like superlattices indicate that not only the disorder but also the symmetry of the unit cell plays a crucial role for enhancing the efficiency. In particular, a giant enhancement is shown for Thue-Morse-like systems when compared with the enhancement for Fibonacci-like superlattices.

DOI: 10.1103/PhysRevB.98.075406

## I. INTRODUCTION

Advances in microstructuring and numerical modeling techniques with detailed fabrication and study of complex photonic structures have led to a considerable body of knowledge about second harmonic generation (SHG) processes in plasmonic systems [1–6] and in periodic [7–9], defective [10–20], disordered [21–24], and dielectric quasiperiodic [25–28] photonic superlattices. This is not the case though for SHG in self-similar plasmonic photonic superlattices, in spite of the possible extension of broadband capabilities in fractal plasmonic systems, which would be useful for ultrabroadband laser sources. Here we present such a study.

The observation of SHG in a quartz crystal pumped by a laser beam [29] has inspired theoretical and experimental work [30,31], with a recent focus on broadening the bandwidth and increasing conversion efficiencies. Proposals for improved conversion efficiencies have been mainly based on strong light localization, with enhanced SHG efficiency at band-gap edges, defective modes, and disordered photonic superlattices [7–24], in addition to the combination with nonlinearities in plasmonic systems [1–6]. To achieve broadbandwidth SHG, on the other hand, photonic superlattices have been designed with multiple reciprocal wave vectors for quasiphase-matching (QPM) condition [15,25,26]. Under this condition, $\Delta k = k_{2\omega} - 2k_{\omega} - G_n = 0$, the wave vectors of SH ($k_{2\omega}$) and fundamental field (FF) ($k_{\omega}$) are related to the reciprocal lattice vector of the photonic structure ($G_n$) to produce high conversion efficiencies. Particularly interesting are the nonlinear quasiperiodic photonic superlattices made with periodic repetition of a unit cell comprising two dielectric building blocks, as reviewed in Ref. [28]. These blocks are arranged as a series of generations according to a given recursion relation to provide different sets of reciprocal wave vectors for the QPM optical parametric process [25–28]. In the linear regime, these quasiperiodic superlattices may display special properties if they include metamaterials, i.e., artificial materials whose properties such as simultaneous negative values for permittivity and permeability [32–47] are not found in naturally occurring materials. Due to the coupling of the longitudinal field component of light with the corresponding plasmonlike effective response of metamaterial layers, the plasmon-polariton (PP) non-Bragg gap was shown to follow the self-similarity properties of the unit cell [48,49], thus being split into a series of PP modes according to the fractal sequence of the unit cell. Analogous self-similarity properties of plasmonic systems have been employed in broadband fractal antennas [50,51].

In this paper, we demonstrate the first highly efficient SHG from self-similar PP band-gap edges in metamaterial quasiperiodic photonic superlattices. This was made by considering quasiperiodic systems with the unit cell built according to the Thue-Morse and Fibonacci fractal sequences illustrated in Fig. 1. These sequences were used in the pioneering works by Merlin *et al.* [52,53] for emphasizing the unique properties of quasiperiodic heterostructures, and recently utilized to demonstrate the quasiperiodic nature of the PP spectra in fractal-like quasiperiodic photonic superlattices [49]. The results discussed here are promising for broadband laser sources [15], frequency multipliers [20], and SHG with low-power lasers [54].

## II. THEORETICAL FRAMEWORK

We consider a finite one-dimensional quasiperiodic multilayer structure made as a periodic repetition of fractal-like elementary cells. The building layers of these elementary units are taken as made of nonlinear dielectric $LiNbO_3$ [15,17] labeled A, and a linear negative-refractive metamaterial, labeled B, alternated according to the Thue-Morse or Fibonacci fractal sequences, as depicted in Figs. 1(a) and 1(b), respectively. For the sake of simplicity we consider hypothetical lossless

*jrmejia3146@gmail.com

 

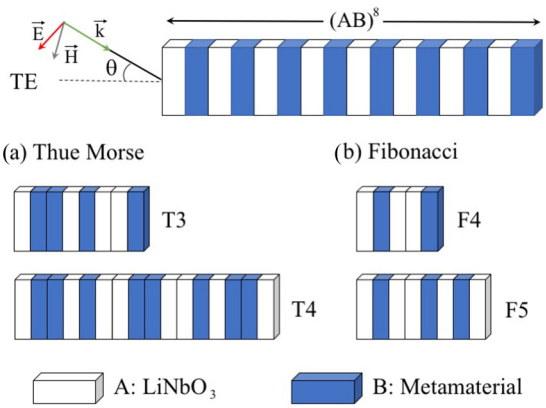


FIG. 1. Pictorial view of (a) Thue-Morse-like and (b) Fibonacci-like building unit cells for the quasiperiodic metamaterial superlattices under study. The upper chart illustrates the incident polarization for a superlattice made by the periodic repetition of eight unit cells AB.

metamaterial slabs, with their permittivity and permeability described by

$$\varepsilon_{\mathrm{B}} = 1 - \frac{\nu_p^2}{\nu^2}, \tag{1}$$

$$\mu_{\mathrm{B}} = 1 - \frac{F\nu^2}{\nu^2 - \nu_0^2}, \tag{2}$$

with $\nu_{\mathrm{p}} = 10$ GHz, $F = 0.56$, and $\nu_0 = 4$ GHz, while the refractive indices for dielectric nonlinear layers are described by $n_{\mathrm{A}}^{(1)} = 2.157$ and $n_{\mathrm{A}}^{(2)} = 2.237$ [12,16] for the FF and SH waves, respectively. The magnetic bulk PP frequency, i.e., the frequency for which $\mu_{\mathrm{B}}(\nu_{\mathrm{m}}) = 0$ is $\nu_{\mathrm{m}} = 6.03$ GHz. The assumption of negligible losses in the microwave regime here is supported by techniques to develop negative refractive metamaterials [42,45,47], while intrinsic ohmic losses of double negative metamaterials at THz regime, associated with metallic building resonators, have been shown to have a detrimental effect on the SHG [19]. The second-order nonlinear susceptibility was taken as $\chi_{\mathrm{B}}^{(2)} = 0$ for linear metamaterial slabs, while $\chi_{\mathrm{A}}^{(2)} = 6.7$ pm/V for nonlinear $LiNbO_3$ slabs at microwave frequencies [55,56]. An incident electric field amplitude $E_0 = 10^7$ V/m (intensity $\sim 13.3\,\mathrm{MW/cm^2}$) was used [9]. In the case of a transversal electric (TE) incident field and growth direction along the $z$ axis (illustrated in the upper chart of Fig. 1), the electromagnetic field propagation is described by the following set of coupled equations [9,16]:

$$\left(\frac{d^2}{dz^2} + (k_{iz}^{(1)})^2\right) E_i^{(1)} = -2(k_0^{(1)})^2 \chi_i^{(2)} E_i^{*(1)} E_i^{(2)}, \tag{3}$$

$$\left(\frac{d^2}{dz^2} + (k_{iz}^{(2)})^2\right) E_i^{(2)} = -(k_0^{(2)})^2 \chi_i^{(2)} (E_i^{(1)})^2, \tag{4}$$

with $\chi_i^{(2)}, k_{iz}^{(j)} = n_i^{(j)} k_0^{(j)} \cos(\theta_i^{(j)}), k_0^{(j)} = \frac{j\omega^{(1)}}{c}, k_{0z}^{(j)} = k_0^{(j)} \cos(\theta_0^{(j)})$, and $\theta_i^{(j)}$ denoting the corresponding second-order nonlinear susceptibility, wave vectors, and propagation angles for FF ($j = 1$) and SH ($j = 2$) waves in the $i$th layer. Under the condition $\frac{|E_i^{(2)}|}{|E_i^{(1)}|} \ll 1$, as in the present case, Eq. (3) can be approximated by [30]

$$\left(\frac{d^2}{dz^2} + (k_{iz}^{(1)})^2\right) E_i^{(1)} = 0, \tag{5}$$

which is known as the undepleted pump approximation, i.e., the amplitude of the SH wave is sufficiently low for the back-coupling to the FF to be neglected. The transfer matrix method (TMM), recently extended to study SHG under oblique incident light in dielectric [16] and metamaterial [19] layers, was used to solve the set of Eqs. (4) and (5). Initial conditions were taken as $E_0^{(2)+} = 0$ and $E_t^{(2)-} = 0$, bearing in mind that there is no incident SH wave. The superindices $+/-$ indicate forward/backward SH waves at the surrounding media. Conversion efficiencies are calculated as $\eta_{\mathrm{f}} = \frac{|E_t^{(2)+}|^2}{|E_0|^2}$ and $\eta_{\mathrm{b}} = \frac{|E_0^{(2)-}|^2}{|E_0|^2}$, for the forward and backward SH waves [17], respectively, while $\eta = \eta_{\mathrm{f}} + \eta_{\mathrm{b}}$ is the total conversion efficiency [7]. Recurrence relations for the transfer matrix of each fractal generation are obtained as $\mathrm{T}_m(\mathrm{A},\mathrm{B}) = \mathrm{T}_{m-1}(\mathrm{A},\mathrm{B})\mathrm{T}_{m-1}(\mathrm{B},\mathrm{A})$ ($m \geqslant 2$), with initial condition $\mathrm{T}_1(\mathrm{A},\mathrm{B}) = \mathrm{AB}$, and $\mathrm{F}_m(\mathrm{A},\mathrm{B}) = \mathrm{F}_{m-1}(\mathrm{A},\mathrm{B})\mathrm{F}_{m-2}(\mathrm{A},\mathrm{B})$ ($m \geqslant 2$), with initial conditions $\mathrm{F}_0(\mathrm{A},\mathrm{B}) = \mathrm{B}$ and $\mathrm{F}_1(\mathrm{A},\mathrm{B}) = \mathrm{A}$, for Thue-Morse-like and Fibonacci-like elementary cells [48,49], respectively. The slab thicknesses were $l_{\mathrm{A}} = l_{\mathrm{B}} = 8$ mm in the calculations, where subindices A and B represent the corresponding layers and $N = 8$ unit cells for all cases, i.e., we considered the superlattices as $[\mathrm{T}_m(\mathrm{A},\mathrm{B})]^N$ and $[\mathrm{F}_m(\mathrm{A},\mathrm{B})]^N$ for each step of the Thue-Morse and Fibonacci sequences.

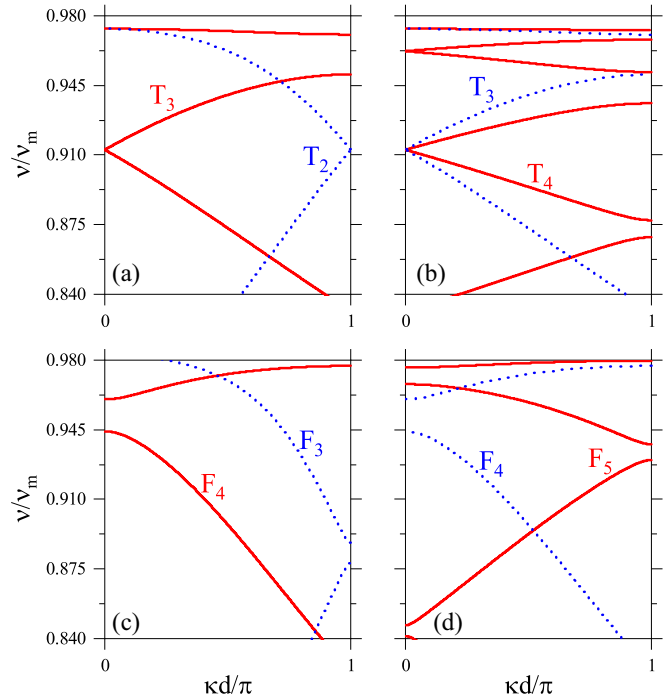


FIG. 2. Comparison of the photonic band structure for Thue-Morse quasiperiodic superlattices (a) $\mathrm{T}_2$ (dotted) and $\mathrm{T}_3$ (solid) and (b) $\mathrm{T}_3$ (dotted) and $\mathrm{T}_4$ (solid). Results for Fibonacci quasiperiodic superlattices are presented for (c) $\mathrm{F}_3$ (dotted) and $\mathrm{F}_4$ (solid) and (d) $\mathrm{F}_4$ (dotted) and $\mathrm{F}_5$ (solid). The alternation of layers A and B in the unit cell follows the corresponding $m$-step of the Fractal sequence, as depicted in Fig. 1.

### III. RESULTS AND DISCUSSION

The rationale in this paper is to exploit the strong light-matter interaction associated with plasmonic resonances, in combination with multiple PP modes in fractal structures, to produce broadband giant SHG enhancement. This concept is demonstrated for two fractal sequences, viz., the Thue-Morse and Fibonacci sequences, with their respective unit cells built by stacking two different slabs, as schematized in Fig. 1. Photonic band structures for the quasiperiodic Thue-Morse and Fibonacci metamaterial superlattices, under oblique incidence ($\theta = 32^\circ$), around the magnetic bulk PP ($\nu/\nu_m = 1$) are shown in Fig. 2. Results are presented for superlattices with unit cells made by following the steps $T_2$, $T_3$, $T_4$ [Figs. 2(a)–2(b)] and $F_3$, $F_4$, $F_5$ [Figs. 2(c)–2(d)] of the Thue-Morse and Fibonacci sequences (see Fig. 1), respectively, indicating an increase in the number of PP modes with increasing steps in the sequences. These PP bands can also be tuned by varying the incidence angle [48,49]. The SH conversion efficiencies, $\eta$, as functions of the incident frequency ($\nu/\nu_m$) are shown in Fig. 3. Peaks in Fig. 3 correspond to either, or both, the FF and the SH waves being band edges, as can be seen from Fig. 4. This behavior is explained in terms of the strong electromagnetic field localization along the structure, supported by calculations in Figs. 5 and 6. These latter figures show sets of localized peaks in FF and SH waves associated with weak disorder effects induced by the fractal aspects [21].

Higher enhancements of the electromagnetic field and $\eta$ in Thue-Morse sequences can be attributed to higher levels of disorder than in Fibonacci lattices [27], reflected in stronger electromagnetic field localization in the structure, as noted from Figs. 5 and 6. Furthermore, theoretical and experimental works demonstrating symmetry-induced linear perfect transmission in quasiperiodic multilayers [57,58]

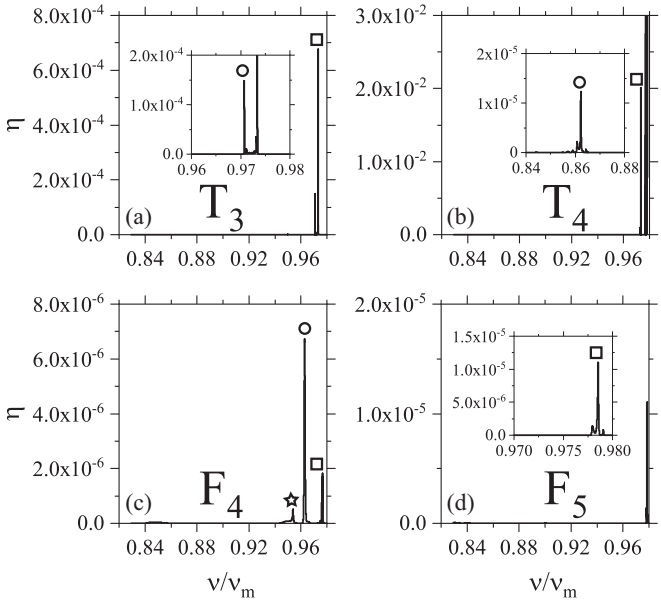


FIG. 3. Efficiencies, $\eta$, for SHG in the PP-gap of Thue-Morse (a) $T_3$, and (b) $T_4$, and Fibonacci (c) $F_4$, and (d) $F_5$ quasiperiodic superlattices. Circles, squares, and stars are used to highlight the corresponding frequencies.

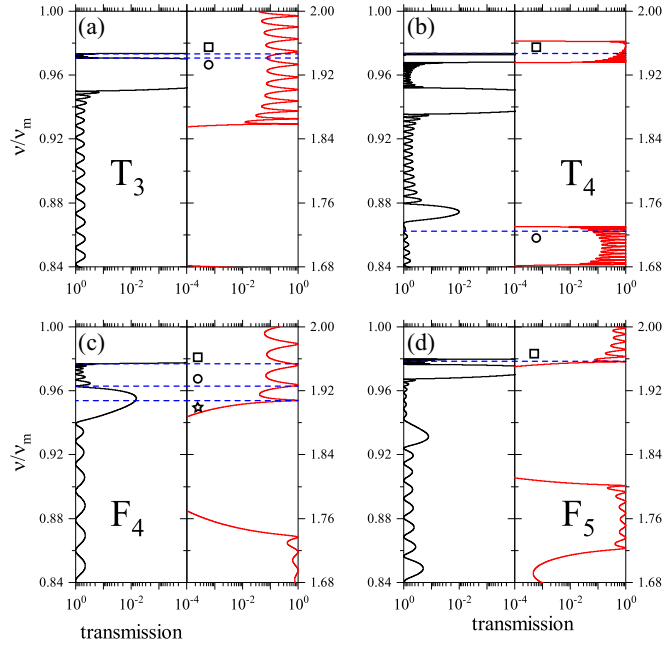


FIG. 4. Transmittance spectra for Thue-Morse (a) $T_3$ and (b) $T_4$, and Fibonacci (c) $F_4$ and (d) $F_5$ quasiperiodic superlattices around the PP gap. Left and right panels of each figure correspond to the FF and SH waves. The alternation of layers A and B in the unit cell follows the corresponding $m$-step of the Thue-Morse and Fibonacci sequences. Dashed lines are used for frequencies associated with the higher peaks marked by circles, squares, and stars in Fig. 3.

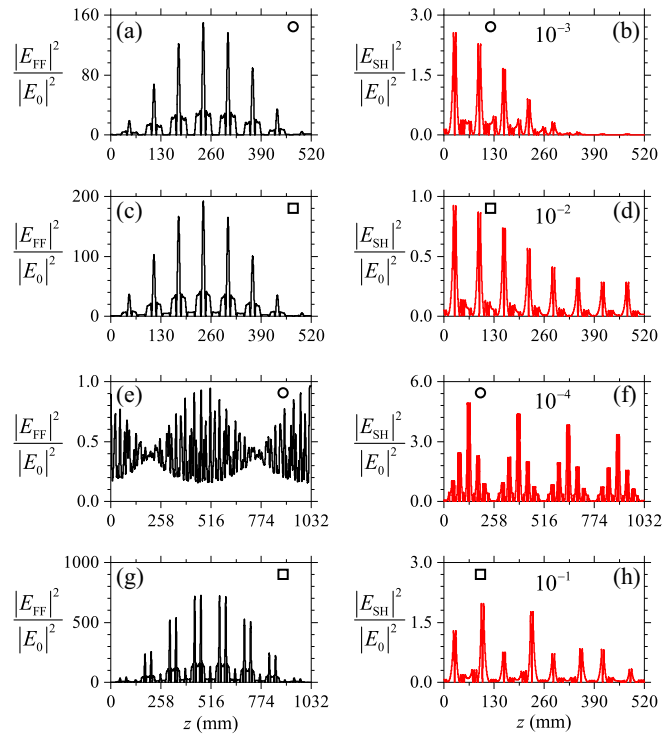


FIG. 5. FF (left panel) and SH (right panel) field profiles are presented for quasiperiodic superlattices following the steps $T_3$ [(a)–(d)] and $T_4$ [(e)–(h)] of the Thue-Morse sequence. The corresponding frequencies are marked by circles and squares according to Figs. 3 and 4.

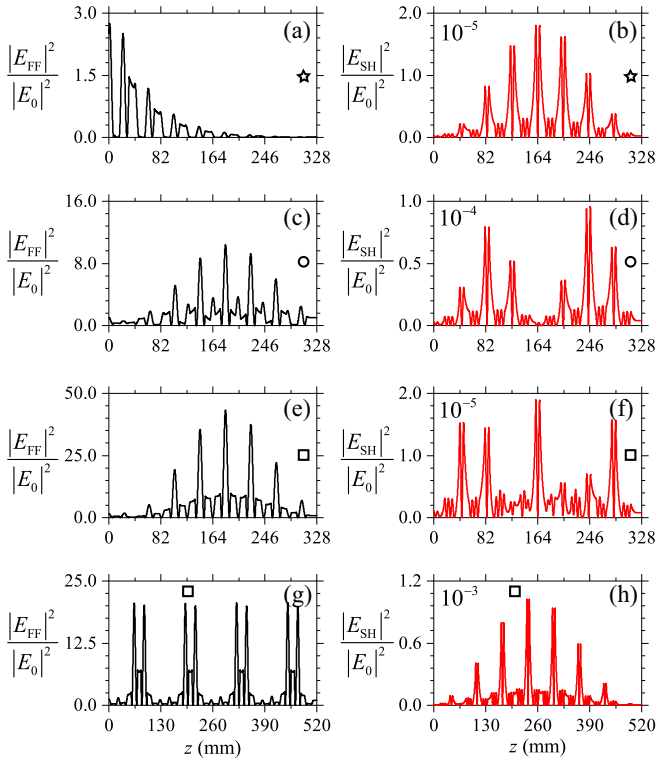


FIG. 6. Field profiles for the FF (left panel) and SH (right panel) waves following the steps $F_4$ [(a)–(f)] and $F_5$ [(g)–(h)] of the Fibonacci sequence. Circles, squares, and stars are used to mark the corresponding frequencies from Figs. 3 and 4.

indicate that symmetry properties of Thue-Morse superlattices can play a crucial role in the enhancement of $\eta$. In particular, Thue-Morse superlattices have a mirror symmetry around a vertical axis along the center of the unit cell for even $m$-values, i.e., $T_2(A, B) = (AB)(BA)$ and $T_4(A, B) = (ABBABAAB)(BAABABBA)$, while an antisymmetric behavior is shown for odd $m$-values, $T_1(A, B) = AB$ and $T_3(A, B) = (ABBA)(BAAB)$.

## IV. CONCLUSIONS

In summary, we have demonstrated large enhancement efficiencies and broadband applicability for SHG in self-similar bulklike PP modes in quasiperiodic superlattices containing double negative metamaterials. The enhancement was illustrated with results for Thue-Morse and Fibonacci-like unit cells. The concepts and superlattice design presented here may have potential applications for multiwavelength laser frequency conversion, even with low-power sources.

## ACKNOWLEDGMENTS

We acknowledge the financial support from the Colombian agency COLCIENCIAS (FP44842-128-2017) and the Brazilian Agencies CNPq and FAPESP (2013/14262-7 and 2016/12311-9). F.R.G. thanks the warm hospitality of University of Cantabria, where calculations in this work were performed.

[1] R. Kolkowski, J. Szeszko, B. Dwir, E. Kapon, and J. Zyss, Opt. Exp. **22**, 30592 (2014).
[2] J. Butet, P.-F. Brevet, and O. J. F. Martin, ACS Nano **9**, 10545 (2015).
[3] S. A. Zolotovskaya, M. A. Tyrk, A. Stalmashonak, W. A. Gillespie, and A. Abdolvand, Nanotechnology **27**, 435703 (2016).
[4] L. Sánchez-García, C. Tserkezis, M. O. Ramírez, P. Molina, J. J. Carvajal, M. Aguiló, F. Díaz, J. Aizpurua, and L. E. Bausá, Opt. Exp. **24**, 8491 (2016).
[5] K. N. Reddy, P. Y. Chen, A. I. Fernández-Domínguez, and Y. Sivan, J. Opt. Soc. B **34**, 1824 (2017).
[6] M. E. Inchaussandague, M. L. Gigli, K. A. O'donnell, E. R. Méndez, R. Torre, and C. I. Valencia, J. Opt. Soc. Am. B **34**, 27 (2017).
[7] N. Mattiucci, G. D'Aguanno, M. J. Bloemer, and M. Scalora, Phys. Rev. E **72**, 066612 (2005).
[8] G. D'Aguanno, N. Mattiucci, M. J. Bloemer, and M. Scalora, Phys. Rev. E **73**, 036603 (2006).
[9] G. D'Aguanno, N. Mattiucci, M. Scalora, and M. J. Bloemer, Phys. Rev. E **74**, 026608 (2006).
[10] B. Shi, Z. M. Jiang, and X. Wang, Opt. Lett. **26**, 1194 (2001).
[11] T. V. Dolgova, A. I. Maidykovski, M. G. Martemyanov, A. A. Fedyanin, O. A. Aktsipetrov, G. Marowsky, V. A. Yakovlev, G. Mattei, N. Ohta, and S. Nakabayashi, J. Opt. Soc. Am. B **19**, 2129 (2002).
[12] F.-F. Ren, R. Li, C. Cheng, and H.-T. Wang, J. Qiu, J. Si, and K. Hirao, Phys. Rev. B **70**, 245109 (2004).
[13] Q. G. Du, F.-F. Ren, C. H. Kam, and X. W. Sun, Opt. Exp. **17**, 6682 (2009).
[14] M. Tlidi, P. Kockaert, and L. Gelens, Phys. Rev. A **84**, 013807 (2011).
[15] B.-Q. Chen, M.-L. Ren, R.-J. Liu, C. Zhang, Y. Sheng, B.-Q. Ma, and Z.-Y. Li, Light: Sci. Appl. **3**, e189 (2014).
[16] H. Li, J. W. Haus, and P. Banerjee, J. Opt. Soc. Am. B **32**, 1456 (2015).
[17] T. S. Parvini, M. M. Tehranchi, and S. M. Hamidi, Appl. Phys. A **118**, 1447 (2015).
[18] Z. Lin, X. Liang, M. Lončar, S. G. Johnson, and A. W. Rodríguez, Optica **3**, 233 (2016).
[19] F. Reyes Gómez, J. R. Mejía-Salazar, O. N. Oliveira Jr., and N. Porras-Montenegro, Phys. Rev. B **96**, 075429 (2017).
[20] M. S. Mohamed, A. Simbula, J.-F. Carlin, M. Minkov, D. Gerace, V. Savona, N. Grandjean, M. Galli, and R. Houdré, APL Phot. **2**, 031301 (2017).
[21] D. Faccio and F. Bragheri, Phys. Rev. E **71**, 057602 (2005).
[22] I. Varon, G. Porat, and A. Arie, Opt. Lett. **36**, 3978 (2011).
[23] Y. Sheng, D. Ma, M. Ren, W. Chai, Z. Li, K. Koynov, and W. Krolikowski, Appl. Phys. Lett. **99**, 031108 (2011).
[24] K. Ren, Y. Liu, X. Ren, and J. Fan, J. Mod. Opt. **63**, 1719 (2016).
[25] Y.-Y. Zhu and N.-B. Ming, Phys. Rev. B **42**, 3676 (1990).
[26] S.-N. Zhu, Y.-Y. Zhu, Y.-Q. Qin, H.-F. Wang, C.-Z. Ge, and N.-B. Ming, Phys. Rev. Lett. **78**, 2752 (1997).
[27] L. Wang, X. Yang, and T. Chen, Physica B **404**, 3425 (2009).

[28] L. Dal Negro and S. V. Boriskina, Laser Photonics Rev. **6**, 178 (2012).
[29] P. A. Franken, A. E. Hill, C. W. Peters, and G. Weinreich, Phys. Rev. Lett. **7**, 118 (1961).
[30] R. W. Boyd, *Nonlinear Optics* (Academic Press, New York, 1992).
[31] Y. R. Shen, *The Principles of Nonlinear Optics* (Wiley Classic Library, Hoboken, NJ, 2003).
[32] V. G. Veselago, Sov. Phys. Usp. **10**, 509 (1968).
[33] J. B. Pendry, A. J. Holden, D. J. Robbins, and W. J. Stewart, IEEE Trans. Microwave Theory Tech. **47**, 2075 (1999).
[34] D. R. Smith, W. J. Padilla, D. C. Vier, S. C. Nemat-Nasser, and S. Schultz, Phys. Rev. Lett. **84**, 4184 (2000).
[35] R. A. Shelby, D. R. Smith, and S. Schultz, Science **292**, 77 (2001).
[36] A. Grbic and G. V. Eleftheriades, J. Appl. Phys. **92**, 5930 (2002)
[37] T. J. Yen, W. J. Padilla, N. Fang, D. C. Vier, D. R. Smith, J. B. Pendry, D. N. Basov, and X. Zhang, Science **303**, 1494 (2004).
[38] S. Linden, C. Enkrich, M. Wegener, J. F. Zhou, T. Koschny, and C. M. Soukoulis, Science **306**, 1351 (2004).
[39] S. Zhang, W. J. Fan, B. K. Minhas, A. Frauenglass, K. J. Malloy, and S. R. J. Brueck, Phys. Rev. Lett. **94**, 037402 (2005).
[40] C. M. Soukoulis, S. Linden, and M. Wegener, Science **315**, 47 (2007).
[41] H. J. Lezec, J. A. Dionne, and H. A. Atwater, Science **316**, 430 (2007).
[42] W. Wu, E. Kim, E. Ponizovskaya, Y. Liu, Z. Yu, N. Fang, Y. R. Shen, A. M. Bratkovsky, W. Tong, C. Sun, X. Zhang, S.-Y. Wang, and R. S. Williams, Appl. Phys. A **87**, 143 (2007).
[43] S. Zhou, S. Townsend, Y. M. Xie, X. Huang, J. Shen, and Q. Li, Opt. Lett. **39**, 2415 (2014).
[44] B. Gong, X. Zhao, Z. Pan, S. Li, X. Wang, Y. Zhao, and C. Luo, Scient. Rep. **4**, 4713 (2014).
[45] D. A. Lee, L. J. Vedral, D. A. Smith, R. L. Musselman, and A. O. Pinchuk, AIP Adv. **5**, 047119 (2015).
[46] S. Lee, B. Kang, H. Keum, N. Ahmed, J. A. Rogers, P. M. Ferreira, S. Kim, and B. Min, Sci. Rep. **6**, 27621 (2016).
[47] H. T. Nguyen, T. S. Bui, S. Yan, G. A. E. Vandenbosch, P. Lievens, L. D. Vu, and E. Janssens, Appl. Phys. Lett. **109**, 221902 (2016).
[48] M. S. Vasconcelos and E. L. Albuquerque, Phys. Rev. B **57**, 2826 (1998).
[49] E. Reyes-Gómez, N. Raigoza, S. B. Cavalcanti, C. A. A. de Carvalho, and L. E. Oliveira, J. Phys.: Condens. Matter **22**, 385901 (2010).
[50] A. A. Omar, Int. J. RF Microwave Comput.-Aided Eng. **23**, 200 (2013).
[51] E. P. Bellido, G. D. Bernasconi, D. Rossouw, J. Butet. O. J. F. Martin, and G. A. Botton, ACS Nano **11**, 11240 (2017).
[52] R. Merlin, K. Bajema, Roy Clarke, F.-Y. Juang, and P. K. Bhattacharya, Phys. Rev. Lett. **55**, 1768 (1985).
[53] Z. Cheng, R. Savit, and R. Merlin, Phys. Rev. B **37**, 4375 (1988).
[54] K. Miyata, F. Rotermund, and V. Petro, IEEE Phot. Tech. Lett. **21**, 1417 (2009).
[55] G. D. Boyd, T. J. Bridges, M. A. Pollack, and E. H. Turner, Phys. Rev. Lett. **26**, 387 (1971).
[56] *Infrared and Millimeter Waves*, edited by K. J. Button (Academic Press, New York, 1983), Vol. 9, Part I, Chap. 3C.
[57] X. Q. Huang, S. S. Jiang, R. W. Peng, and A. Hu, Phys. Rev. B **63**, 245104 (2001).
[58] R. W. Peng, X. Q. Huang, F. Qiu, Mu Wang, A. Hu, and S. S. Jiang, Appl. Phys. Lett. **80**, 3063 (2002).